Investigation of repair techniques for deteriorated end regions of prestressed concrete bridge girders

William B. Rich, Christopher S. Williams, and Robert J. Frosch

- Deterioration of the end regions of prestressed concrete bridge girders is commonly observed in the field when girders are exposed to chloride-laden water that has leaked through failed expansion joints.
- Reliable repair techniques can provide a means to extend girder service life, avoiding the need for immediate superstructure replacement. Three repair systems were evaluated, but only the externally bonded FRP system successfully restored both the strength and initial stiffness of the girder.
- The tests also demonstrate that end region deterioration can cause significant reductions in strength, underscoring the importance of addressing such deterioration observed in the field.

Reliable, cost-effective repair solutions for bridge structures are essential for transportation agencies managing aging infrastructure or bridges experiencing premature deterioration. When damage is concentrated within localized regions, repair options that restore the performance of deteriorated components are attractive because they are less disruptive and less expensive than the replacement of entire bridge components. Furthermore, repair solutions that minimize or eliminate road closures enhance the safety of the traveling public.

In areas with relatively harsh winter conditions, the end regions of prestressed concrete superstructure girders are an example of localized regions of bridge components that often experience premature deterioration.[1–8] If chloride-laden water forms through the use of deicing salt and leaks through failed expansion joints in the deck or between the deck and approach slab, the end regions of the girders below the joints are then exposed to the chloride-laden water, leading to a corrosive environment in which concrete spalling and reinforcement section loss occur (**Fig. 1**).[1,2,6–8] Cycles of freezing and thawing can exacerbate deterioration.[1,6,7] Given the frequency with which bridges with end region deterioration are observed and the fact that the deterioration is often localized to the end region of the girders, a repair technique is needed that can effectively extend the service life of these bridges, avoiding the need for superstructure replacement.

Deterioration of bottom flange

Deterioration within web

Figure 1. Prestressed concrete bridge girders with end region deterioration.

Previous research on repair methods

Few studies have evaluated potential methods for the repair of deteriorated end regions of prestressed concrete girders to restore the strength and stiffness of the components. The primary techniques that researchers have explored can be divided into two categories: applying fiber-reinforced-polymer (FRP) systems and fabricating a concrete end block that encases the damaged region.

FRP systems

FRP systems have a high strength-to-weight ratio, are naturally corrosion resistant, come in a variety of materials (carbon, glass, and aramid), and have high installation flexibility.[9–12] Two common applications of FRP for the repair and strengthening of structural concrete components are externally bonded and near-surface-mounted (NSM) systems. Externally bonded FRP consists of fibers and resin combined to form a laminate that is applied to the surface of a concrete component with an adhesive. NSM reinforcement consists of FRP bars or strips installed in grooves cut into the surface of a concrete component.[9] Although the use of FRP as a repair and strengthening system has been widely studied, relatively few researchers have explored the use of FRP systems specifically for repairing deteriorated end regions of bridge girders.[1,5,6,13]

Petty et al.[5] studied the effectiveness of different externally bonded FRP configurations on deteriorated end regions of American Association of State and Highway Transportation Officials (AASHTO) Type II prestressed concrete girders that were salvaged from two bridges. After evaluating five carbon-fiber-reinforced polymer (CFRP) repair configurations through shear tests on repaired girders, the authors concluded that the configuration consisting of U-wrap sheets with fibers on the side faces of the girder oriented 90 degrees relative to the longitudinal axis of the component combined with longitudinal CFRP strips used to anchor the U wraps was the most effective because of its "increases in shear, consistency, ease of application, and simplicity of design."[5]

Ramseyer and Kang[6] examined the effectiveness of externally bonded glass-fiber-reinforced polymer (GFRP) and CFRP for repairing AASHTO Type II prestressed concrete girders that had been damaged in the laboratory by failing the girder ends in shear prior to repair. After rapid-set cement was added to replace concrete missing because of the shear failures, FRP was installed in a U-wrap configuration. Cracks were also injected with epoxy on select beam ends. The only repair system that successfully restored the shear strength of the end region was GFRP with epoxy-injected cracks; however, the authors concluded that the CFRP recovered more stiffness than the GFRP.

Andrawes et al.[1] also evaluated end region repairs using FRP on AASHTO Type II prestressed concrete girders. The specimens were damaged by mechanically removing the concrete cover within the end regions of the components. For a full-scale girder receiving an externally bonded FRP repair, rapid-set mortar was first used to restore the girder cross section. Vertically oriented CFRP sheets were then applied to the sides of the girder, and longitudinal strips were used to anchor these vertical sheets, a configuration similar to that studied by Petty et al.[5] The repair system resulted in the shear capacity and ductility of the specimen exceeding those of an undamaged control girder; however, a specimen repaired with mortar alone did not restore the strength or ductility to that of the control specimen. Andrawes and colleagues[1] also evaluated an NSM FRP repair system in small-scale girders, but the system was unsuccessful in restoring the shear capacity to that of an undamaged specimen.

Concrete end block

The fabrication of a concrete end block within the damaged end region is another technique that has been implemented to repair prestressed concrete bridge girders with end region deterioration.[2–4,8] End block repairs increase the size of the original cross section of the girder and rely on supplemental mild reinforcement or concrete anchors to transfer stresses from the original cross section into the concrete end block.

Needham[3,4] described the development and implementation of an end block repair procedure for the deteriorated end regions of prestressed concrete I-beams of an in-service bridge. A latex-modified concrete was used to form the end block. Although several problems arose during the girder repairs that were performed in the field, the repair procedure was considered a cost-effective method for extending the service life of deteriorated girders.[4]

Shield and Bergson[8] examined the performance of end blocks formed using shotcrete that were added to in-service prestressed concrete I-shaped girders with significant end region deterioration. Approximately 3.5 years after the end blocks were added, the repaired girders were removed from the bridge and load tested in shear. They failed at slightly greater loads than undamaged companion specimens extracted from the same bridge, demonstrating the success of the repair.

Floyd et al.[2] investigated end region repair using ultra-high-performance concrete (UHPC), fiber-reinforced self-consolidating concrete (SCC), and magnesium-alumino-liquid-phosphate concrete. Six specimens were loaded to failure in shear and then repaired using one of the specialty concrete types to cast a thickened region at the ends of the damaged prestressed girders. Shear tests on the repaired end regions resulted in greater strengths than the capacities achieved during the initial tests. Despite having a smaller thickness, the UHPC repair provided the greatest increase in strength compared with the other two materials.

Research scope and significance

While the results of past research investigating potential end region repair methods have been promising, studies on girders with deterioration from decades of service in the field are limited, and no study has directly compared FRP and end block repair procedures. To compare different repair methods and identify key design considerations for end region repair, an experimental program was conducted on prestressed concrete girders obtained from a decommissioned superstructure. More specifically, three repair techniques were investigated: an externally bonded FRP system, an NSM FRP system, and a concrete end block. Shear tests were performed to evaluate the performance of each repair. The inclusion of three different techniques within the same study allowed the relative effectiveness of each method to be established. The evaluation of each technique applied to 30-year-old, full-scale girders with severe end region deterioration offers valuable insights for developing repair techniques that can be implemented in the field.

Experimental program

Specimen overview

For the experimental program, five decommissioned AASHTO Type I precast, prestressed concrete bridge girders were salvaged from a bridge located on Interstate 469 near Fort Wayne, Ind., that was constructed in 1988. Many of the bridge girders showed signs of significant end region deterioration (Fig. 1). Given the condition of the girders, the bridge superstructure was replaced in 2018, at which time five girders were extracted from the bridge for testing in the laboratory.

Figure 2 shows details of the test specimens. Each specimen was 38.5 ft (11.7 m) long. The AASHTO Type I girders were composite with the original reinforced concrete deck, which had a nominal thickness of 8 in. (200 mm). A thin epoxy overlay had been applied to the top surface of the deck. As specified in the bridge plans,[14] the girders were prestressed with eight 0.5 in. (12.7 mm) diameter seven-wire prestressing strands with an ultimate tensile strength f_{pu} of 270 ksi (1860 MPa). Four of the eight prestressing strands were straight and located 2 in. (50 mm) from the bottom surface of the beam. The remaining four strands were harped with harping points located at one-third of the girder length from each end. All prestressing strands were initially stressed to 189 ksi (1300 MPa), or $0.7f_{pu}$. Figure 2 shows the spacing used for the stirrups, which were fabricated from no. 4 (13M) deformed reinforcing bars. The specified 28-day concrete compressive strength f_c' was 5000 psi (34.5 MPa).[14]

When extracting the girders from the bridge, longitudinal cuts were made approximately 2 in. (50 mm) from the edge of the top flange (Fig. 2). The portion of the deck that remained on the girder was kept in place for the experimental program. A transverse edge beam had been cast monolithically with the deck and extended across the width of the bridge through the 6 in. (150 mm) notch in the elevation (Fig. 2). A portion of this edge beam remained on all test girders except one. A gray patch material was applied to the deteriorated end of

Table 1. Specimen details

Girder	End region condition	Repair technique
C	Good	Control
D	Deteriorated	Tested in damaged condition
R-EXT	Deteriorated	Externally bonded FRP
R-NSM	Deteriorated	NSM FRP
R-BLK	Deteriorated	End block

Note: FRP = fiber-reinforced polymer; NSM = near-surface-mounted.

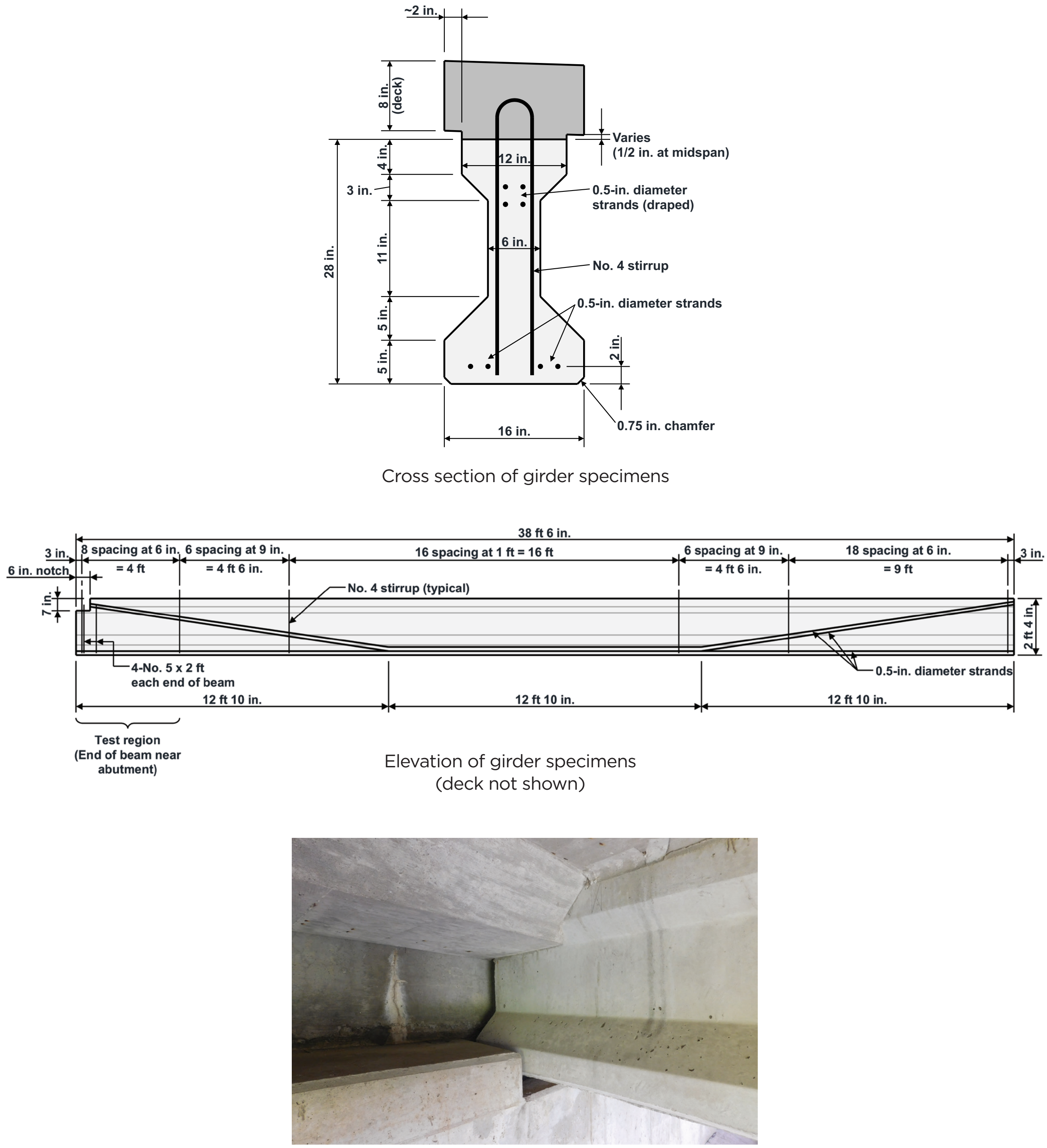

Cross section of girder specimens

Elevation of girder specimens (deck not shown)

Edge beam at ends of girders

Figure 2. Girder details. Source: drawings adapted from Indiana Department of Highways, 1987. Note: 1 in. = 25.4 mm; 1 ft = 0.305 m.

some bridge girders while in service (Fig. 1). This measure is assumed to have been performed to mitigate corrosion.

Table 1 presents the test matrix for the five girder specimens. One of the five test girders, girder C (control), had an end region in good condition and was used as a control specimen. The other four girders exhibited severe end region deterioration. Girder D (damaged) was tested to evaluate the performance of a deteriorated girder in its field condition. The three remaining test specimens, girders R-EXT, R-NSM, and R-BLK (where R is repaired, EXT is externally bonded FRP system, NSM is NSM FRP system, and BLK is concrete end block), were repaired using three techniques (Table 1). For the externally bonded FRP and NSM FRP repairs, the girder cross section within the end region was restored using mortar before the FRP was applied.

Test setup and procedure

Figure 3 shows the test setup for the experimental program. Each girder was loaded in shear with a point load applied 45 in. (1140 mm) from the centerline of the support located at the end of the girder. The relatively short shear span was selected based on the observation that direct compressive stresses transferred from the load to the support would be critical for the end regions. The original elastomeric bearing pads acquired from the bridge were used to support the specimens. Because the top surface of the deck was sloped, gypsum cement was used to cast a thin wedge-shaped block at the load point to provide a level loading surface. A steel loading plate was placed on top of the gypsum wedge. A 5 ft (1.5 m) overhang was provided at the right end of the girder (Fig. 3) to ensure that this end of the girder remained unloaded, allowing the overhanging portion to be tested at a future date if needed.

A hydraulic cylinder applied load to the specimens, and the load was measured using a 300 kip (1330 kN) capacity load cell that was installed in line with the hydraulic cylinder. At the load point and at midspan, linear string potentiometers were used to measure deflections. Additional linear potentiometers were placed to measure displacement at each side of both bearing pads to capture deflections at the supports.

Each test specimen was loaded monotonically to failure. Failure of the test specimens was defined by either a sudden loss in load-carrying capacity or when the applied shear had decreased by at least 20 kip (89 kN) from its maximum value.

Repair systems

Externally bonded FRP system For the externally bonded FRP repair system applied to girder R-EXT, carbon-fiber fabric was selected because it offers both a high ultimate tensile strength and a high elastic modulus and has been demonstrated to be an effective material for the repair and strengthening of concrete structures.[1,5,9,15] Given the bond-critical nature of the externally bonded laminate within the end region of the girder, special consideration was given to the proper anchorage of the FRP reinforcement. FRP spike anchors (also known as FRP fan anchors) were used in the design of the repair system. A spike anchor consists of a bundle of FRP fibers that are inserted into an anchor hole in the concrete substrate and bonded to the primary FRP reinforce-

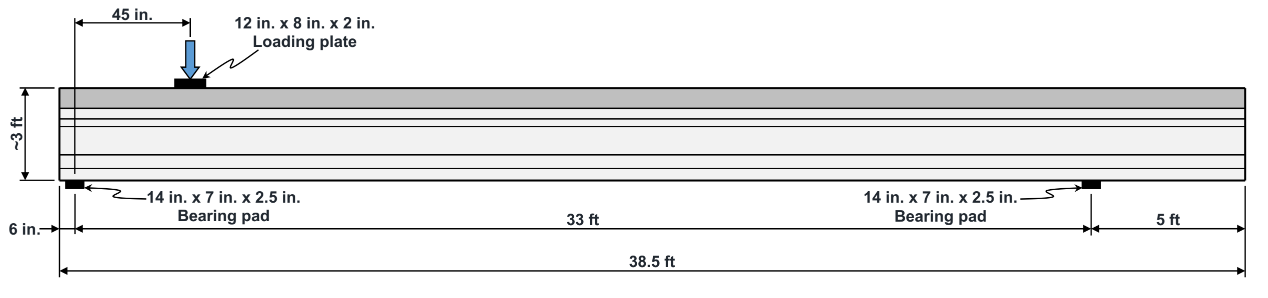

Figure 3. Loading configuration. Note: 1 in. = 25.4 mm; 1 ft = 0.305 m.

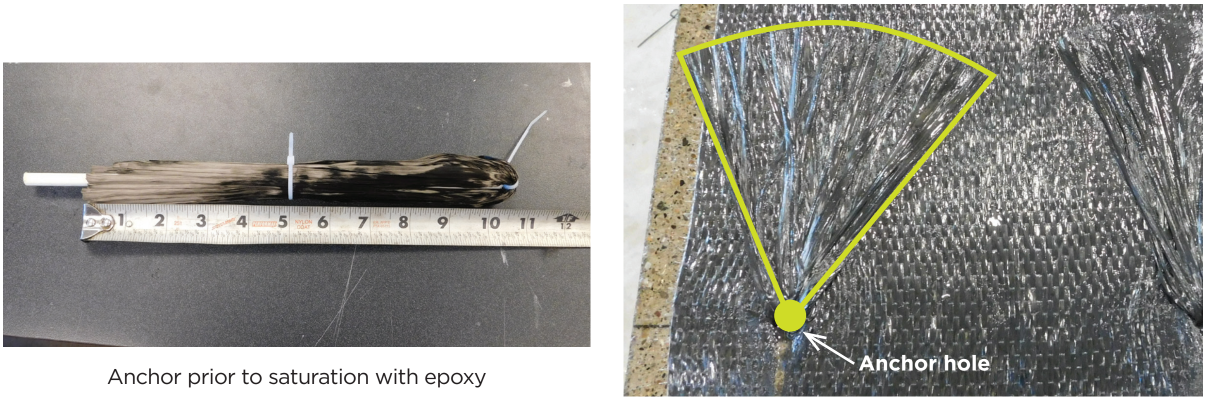

Anchor prior to saturation with epoxy

Installed anchor

Figure 4. Fiber-reinforced-polymer spike anchor.

ment (**Fig. 4**). FRP spike anchors have been shown to provide a reliable means of anchoring externally bonded FRP laminates when it is not possible to wrap the FRP around the entire component. When properly detailed, FRP anchors can develop the full strength of the primary FRP laminate, allowing the fracture capacity of the laminate to be reached.[15,16]

The externally bonded CFRP fabric was combined with an epoxy to form the laminate that was adhered to the concrete surface. The FRP spike anchors were cut from a premanufactured CFRP rope produced by the same manufacturer as the primary FRP reinforcement and were combined with the same epoxy as the CFRP fabric. **Table 2** provides the applicable design properties of the externally bonded FRP reinforcement (FRP strips and sheets) and anchors, both in the form of a cured laminate (except as noted for ultimate rupture strain ε_{fu}^* of the FRP anchor).

Figure 5 shows details of the externally bonded FRP repair system. The repair system was composed of three layers of FRP. The first layer consisted of FRP sheets that were cut into strips and applied with the fibers running parallel to the longitudinal axis of the girder. The second layer consisted of FRP sheets with fibers oriented vertically on the side surfaces of the girder. Spike anchors were used to anchor the longitudinal strips and vertical sheets. The third layer of FRP consisted of externally bonded FRP patches installed over the FRP anchors.

Longitudinal FRP strips were installed as the first layer because of the importance of restoring the tensile capacity of the girder caused by deterioration of the prestressing strands, especially along the bottom flange. This first layer consisted of three strips (Fig. 5). A continuous strip that wrapped around the end of the girder was applied both to the vertical surface of the bottom flange and to the girder web. Continuous strips were used to improve the anchorage of the strips and provide confinement to the mortar used to restore the girder cross section within the end region. Continuous strips are possible because space is typically available behind the girders in the field. These longitudinal strips were anchored at the ends using FRP spike anchors. The longitudinal strips applied to the sloped surface of the bottom flange were two discrete strips on either side of the girder. These strips were not anchored with spike anchors. For bridge girders that contain multiple layers of prestressing strands in the bottom flange, drilling anchor holes perpendicular to the sloped surface presents a high risk of hitting prestressing stands.

The second FRP layer with fibers oriented vertically on the side surfaces of the girder aided with the anchorage of the longitudinal strips of the first layer and added tensile strength in the vertical direction. The two sheets located farthest from the end of the girder were installed in a U-wrap configuration; however, the sheet closest to the end of the girder was a face-bonded sheet that did not wrap around the bottom of the girder due to the support bearing that would be present during in-field installations. Following the recommendations of the manufacturer and research conducted by Andrawes et al.,[1] a minimum 1 in. (25 mm) space was provided between all externally bonded FRP sheets. The 10 in. (250 mm) width of the U-wrap sheets was selected based on practical limits and the results of tests conducted by Pudleiner[17] on specimens with 10 in. wide sheets anchored with two spike anchors. Because the layout of the internal steel at the end of the girder controlled the locations of the spike anchors, the width of the face-bonded sheet was reduced to 5 in. (130 mm), and the space between the face-bonded sheet and the adjacent U-wrap sheet was increased to 2.25 in. (57.2 mm). FRP spike anchors were provided near the ends of each sheet and at the reentrant corner between the bottom flange and the web.

The order with which the first two layers of FRP were applied in this experimental program was different from the order used for systems investigated by Andrawes et al.[1] and Petty et al.[5] in which longitudinal strips were used to anchor vertical sheets. The reason for deviating from these schemes was the importance placed in this study on providing longitudinal tensile capacity in the bottom flange. Given this priority, placing longitudinal strips in the first layer was deemed to be important.

Table 2. FRP repair system components and properties

FRP repair system	Component	Constituent materials	Nominal ply thickness, in.	Cross-sectional area, in.^{2}	f_{fu}^*, ksi	ε_{fu}^*	E_f, ksi
Externally bonded carbon FRP	Externally bonded FRP strips and sheets (laminate)	FRP fabric and epoxy	0.04	n/a	160.9	0.0145	10,390
	FRP anchors (laminate)	FRP rope and epoxy	n/a	0.1†	304	0.016‡	33,300
NSM carbon FRP	NSM strip	FRP tape	n/a	0.049	325	0.0181	18,000

Note: E_f = tensile modulus of elasticity of FRP reinforcement; f_{fu}^* = ultimate tensile strength of FRP reinforcement; FRP = fiber-reinforced polymer; n/a = not applicable; NSM = near-surface-mounted. ε_{fu}^* = ultimate rupture strain of FRP reinforcement. 1 in. = 25.4 mm; 1 in.^{2} = 645 mm^2; 1 ksi = 6.895 MPa.

†Based on single rope segment; assumes 50% fiber content.

‡Based on dry fibers, not the cured laminate.

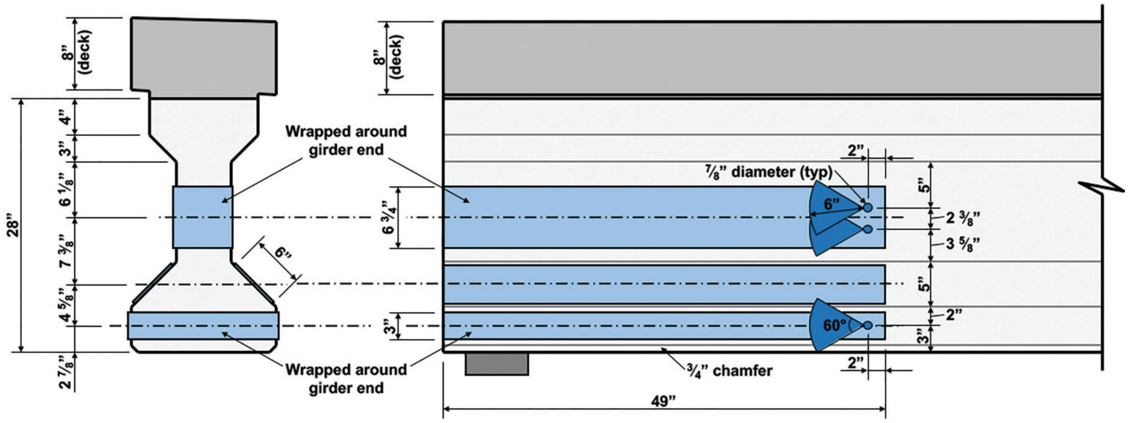

First layer (longitudinal strips)

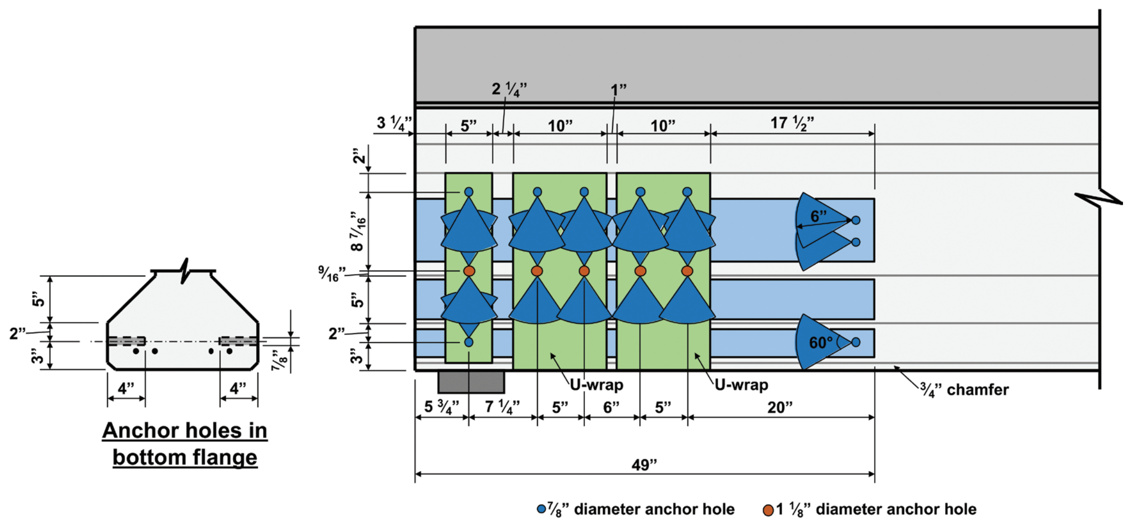

Second layer (vertical sheets)

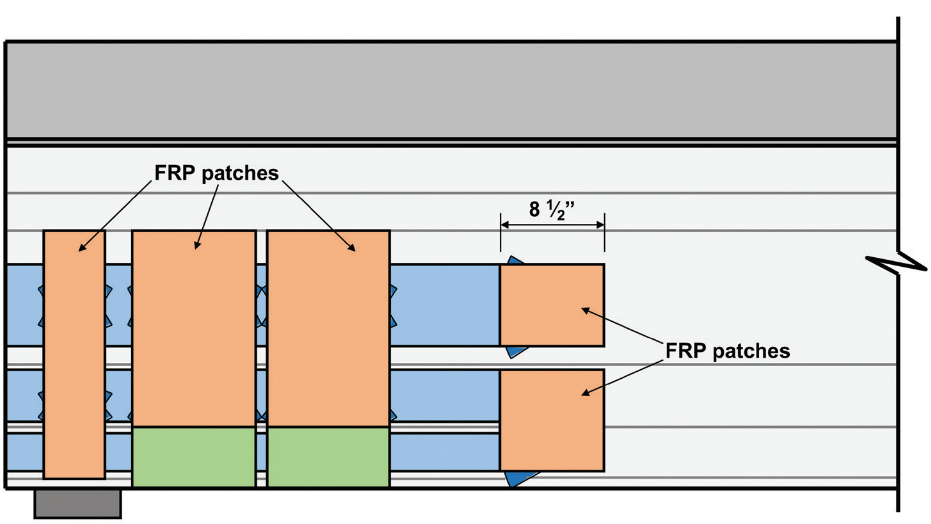

Third layer (patches)

Figure 5. Externally bonded fiber-reinforced polymer (FRP) details for girder R-EXT. Note: 1" = 1 in. = 25.4 mm.

Nineteen FRP spike anchors were used on each side of the girder to anchor the externally bonded strips and sheets (Fig. 5). The design of the anchors was based on recommendations developed by previous researchers.[16–19] The anchor holes in the bottom flange of the girder were placed such that the holes would be positioned between the first and second rows of prestressing strands considering the typical 2 in. (50 mm) strand grid pattern. For these holes, an anchor hole depth of only 4 in. (102 mm) was selected to minimize the risk associated with drilling holes in the bottom flange near prestressing strands. For anchors installed on opposite sides of the girder web, it was not feasible to drill separate anchor holes into each side of the 6 in. (152 mm) thick web of the specimens. Therefore, anchor holes were drilled through the entirety of the web and continuous anchors cut from the FRP rope material were installed in the holes and fanned out on both sides of the girder. A fan angle of 60 degrees was selected for all spike anchors, and the splayed (fan) portion of each anchor was 6 in. (150 mm) long. The number of anchors across the width of each strip and sheet, the required anchor weight and area, and the anchor hole diameter followed the recommendations and calculations outlined by Pudleiner.[17] Considering the area of a single FRP rope segment (Table 2), each spike anchor had a cross-sectional area of approximately 0.31 in.^{2} (200 mm^2) and was formed by combining FRP fibers from multiple rope segments. Rich et al.[12] provides further information about the selected details of the spike anchors.

The third FRP layer of the repair system consisted of externally bonded FRP patches applied over the spike anchors (Fig. 5). Previous investigations have found that such patches help transfer stresses between the FRP strips or sheets and the spike anchors,[16,17] and the patches used in this study consisted of the same fabric and epoxy used for the primary strips and sheets. Based on the results of previous research,[16,17] two layers of patches were placed over the anchors. The fibers of the first layer were orientated perpendicular to the fibers of the externally bonded strip or sheet, and the fibers of the second layer were orientated parallel to the fibers of the externally bonded strip or sheet.

NSM FRP system The NSM FRP system applied to girder R-NSM was designed in an effort to reestablish tensile capacity along the bottom flange of the girder within the end region that had been lost due to strand deterioration and to evaluate whether simply providing this tensile strength would be sufficient to restore the performance of the component. Furthermore, using NSM FRP may be an attractive option because installing NSM reinforcement can be easier than installing the strips, sheets, and anchors of the externally bonded system. As with the externally bonded system, the selected NSM strips were manufactured from carbon fibers. Table 2 provides design properties of the NSM strips. The nominal cross-sectional dimensions of the strips were 0.079 × 0.63 in. (2.0 × 16 mm), and each strip had a nominal area of 0.049 in.^{2} (31.67 mm^2).

Figure 6 shows details of the NSM FRP repair system used for the experimental program. The system consisted of eight NSM FRP strips installed in grooves that were cut within the bottom flange along the sides of the girder. Although ACI PRC-440.2R-17[9] suggests a groove depth of at least 0.95 in. (24 mm) for the NSM strips, this study used a depth of 0.875 in. (22.2 mm) to maintain a groove depth less than the clear cover of 1 in. (25 mm) that is typical for girders with confinement reinforcement enclosing pretensioned strands in the bottom flange within the end region. The clear spacing between the grooves and clear edge distance was also limited by the geometry of the girder and less than the recommendations in ACI PRC-440.2R-17. These limitations, however, are representative of actual field conditions.

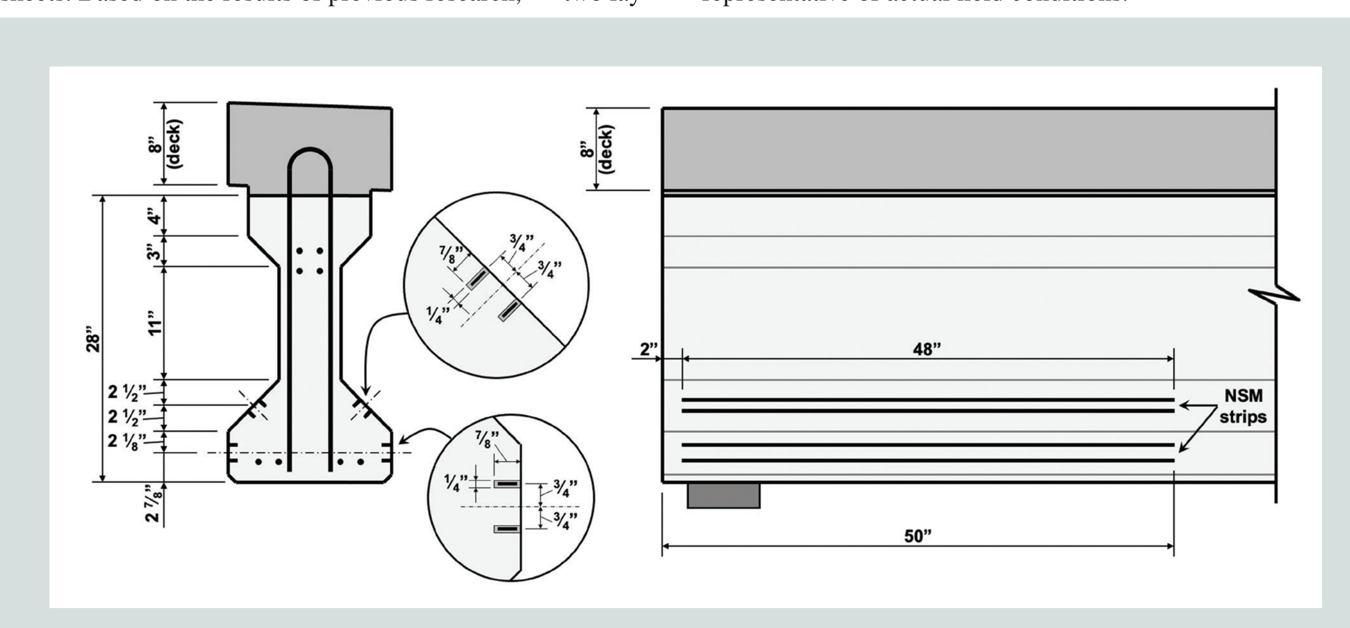

Figure 6. Near-surface-mounted (NSM) fiber-reinforced polymer details for girder R-NSM. Note: 1" = 1 in. = 25.4 mm.

End block system The intention of the end block repair for girder R-BLK was to provide an alternative load path for the most deteriorated portion of the girder, allowing load to transfer to new bearings located away from the original support bearing where concrete was severely deteriorated. **Figure 7** presents details of the end block repair system. The repaired region extended 24 in. (610 mm) along the length of the girder, which was the minimum length needed to repair the portion of the girder that experienced significant section loss. All reinforcement within the end block was Grade 60 (414 MPa) epoxy-coated bars conforming to ASTM A615.[20] An epoxy anchoring gel was used to install four no. 3 (10M) reinforcing bars into holes drilled through the web of the girder, and these reinforcing bars acted as dowels to aid in the transfer of stresses from the web to the new concrete of the end block. To attain the shape in Fig. 7, one end of each no. 3 (10M) bar had to be bent after the bar was inserted through the web. The remainder of the reinforcing cage consisted of no. 4 (13M) bars. The end block was designed with the assumption that the ability to lift the girder from its original elevation would not be possible in the field and that geometric constraints would not allow reinforcement to pass under the bottom surface of the girder.

To account for severe deterioration at the original bearing location, a bearing pad was not placed at this original location during testing, simulating the complete loss of bearing capacity at the original support. Instead, two bearing pads with widths equal to half of the 14 in. (360 mm) width of the original bearing pad (measured transverse to the longitudinal axis of the girder) were placed under the end block (Fig. 7).

It was anticipated that properly vibrating concrete during casting of the end block in the field would be difficult due to limited access at the girder ends. Therefore, SCC was used to cast the end block. **Table 3** presents the SCC mixture proportions.[21,22] The SCC had a 28-day design strength of 6000 psi (41 MPa). A 6 in. (150 mm) clearance was left between the

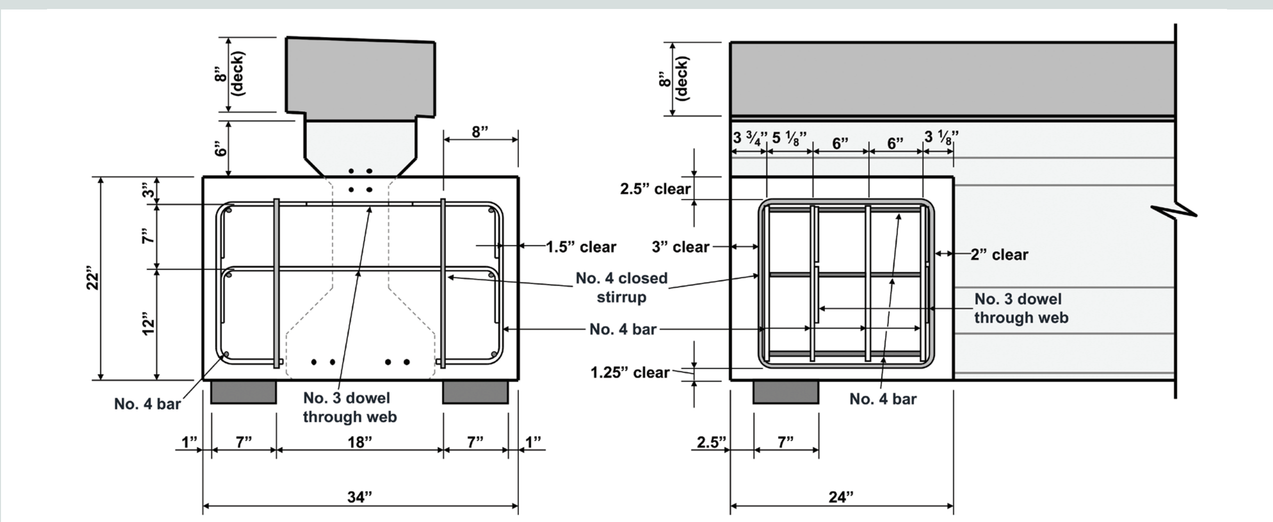

Figure 7. End block details for girder R-BLK. Note: no. 3 = 10M; no. 4 = 13M; 1” = 1 in. = 25.4 mm.

Table 3. Self-consolidating concrete mixture proportions for end block

Material	Details	Design quantity
Cementitious materials	ASTM C150[21] Type 1 cement	580 lb/yd³
	ASTM C618[22] Class F fly ash	145 lb/yd³
Coarse aggregate	⅜ in. pea gravel	1650 lb/yd³
Fine aggregate	Natural sand	1379 lb/yd³
Water	n/a	279.5 lb/yd³
Admixtures	High-range water-reducing admixture	72.5 oz/yd³
	Viscosity modifier	29.0 oz/yd³
Water-cement ratio	n/a	0.39

Note: n/a = not applicable. 1 in. = 25.4 mm; 1 oz/yd³ = 38.681 mL/m³; 1 lb/yd³ = 0.593 kg/m³.

top of the end block and the top surface of the precast concrete girder (Fig. 7) to provide sufficient space for the SCC to be pumped into the top of the forms during field implementation.

Repair procedures

Control specimen The control specimen (girder C) was in good condition, with the only notable sign of destress being cracking in the bottom flange near the end of the girder. No repairs were made. The bearing pad was shifted 3 in. (76 mm) relative to its original location (**Fig. 8**) to avoid the cracks. The shear span remained at a length of 45 in. (1140 mm) (Fig. 3).

Damaged specimen Girder D was tested to evaluate the performance of a deteriorated girder that was left unrepaired after being extracted from the bridge; however, given the severe deterioration of girder D, minimal repairs were required to reestablish the bearing area of the girder (**Fig. 9**) to permit testing. This was accomplished with the application of a prepackaged 6500 psi (45 MPa) fast-setting mortar mixture with low-shrinkage characteristics. To minimize the extent of the repair, the location of the bearing pad was shifted into the girder span by 4 in. (100 mm) from its original location while the shear span of the girder remained at 45 in. (1140 mm) (Fig. 3).

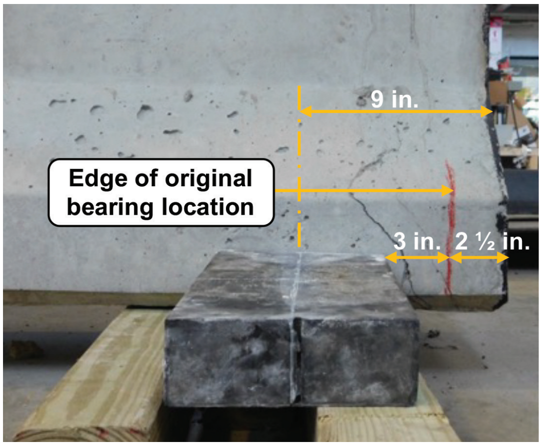

Figure 8. Shifting bearing pad for girder C. Note: 1 in. = 25.4 mm.

Externally bonded FRP repair During the repair procedures for both girders R-EXT and R-NSM, efforts were made to simulate conditions that would be present in the field. Because lifting the ends of the girders in the field would not be possible, bearing pads were placed at their original locations as the repairs were performed. Furthermore, a plywood board was placed approximately 2 in. (50 mm) from the end of the girders to represent a mud wall and provide another realistic constraint (**Fig. 10**).

Figure 10 presents the progression of the repair for girder R-EXT. The repair began by using an electric chipping hammer to remove delaminated and loose concrete from the end region until sound concrete was reached. The regions where concrete was removed or had previously fallen from the specimen were then sandblasted to remove corrosion product and mitigate microcracking caused by the chipping hammer. Next, the original cross section of the girder was restored by applying the same fast-setting mortar used to reestablish the bearing area of girder D. After the mortar cured, the surface of the concrete and mortar to which FRP was to be applied was sandblasted to a concrete surface profile of 3, as defined in the International Concrete Reinforcing Institute's ICRI 310.2R-2013[23] and recommended by ACI PRC-440.2R-17.[9] Anchor holes were then drilled at the locations in Fig. 5. In accordance with ACI PRC-440.2R-17, the edges of the anchor holes and the corners of the girder around which FRP strips and sheets were to be wrapped were rounded to a radius of 0.5 in. (13 mm) to reduce stress concentrations in the FRP.

Prior to repair of bearing area

After mortar repair of bearing area

Girder D prior to testing

Figure 9. Reestablishing bearing area of girder D.

Deteriorated end region | After mortar repair | Completed FRP repair

Figure 10. Progression of externally bonded fiber-reinforced polymer (FRP) repair for girder R-EXT.

Before the FRP reinforcement was installed, the surface of the concrete was primed and sealed using the appropriate epoxy. As recommended by the manufacturer of the FRP reinforcement, a different epoxy resin was used to prepare the concrete than was used to saturate the FRP strips, sheets, and spike anchors to improve the tack of the concrete surface during vertical and overhead applications. After the surface of the girder was prepared, the three layers of FRP were sequentially installed (Fig. 5). Before the FRP strips and sheets were installed, they were saturated with epoxy using plastic laminating rollers. Once the FRP strips and sheets were in place on the concrete surface, the rollers were used to fully impregnate them with epoxy and eliminate air voids. Plastic squeegees were then used to remove excess epoxy.

Next, the spike anchors were installed. For each anchor, a razor blade was used to separate the fibers of the FRP sheets installed on the girder to expose the anchor hole. A caulk dispensing gun was used to inject epoxy into the hole. The spike anchor was saturated with epoxy before installation. Wooden dowels fastened to the anchor with zip ties were used to help insert the anchors into the holes. After an anchor was inserted, the dowel was removed from the anchor hole and the end of the spike anchor extending from the hole was fanned out at a 60-degree angle. The anchor was checked to ensure that it was fully impregnated with epoxy. For the anchors extending through the girder web, both ends of the anchor were fanned out on the sides of the girder. Last, additional epoxy was injected into the anchor holes to eliminate possible air voids. Rich et al.[12] provides the detailed procedure for installing the spike anchors. The FRP patches were installed with the same procedure used for the FRP strips and sheets. Figure 10 shows the completed externally bonded FRP repair system on girder R-EXT.

NSM FRP repair **Figure 11** shows the repair procedure for girder R-NSM. First, unsound concrete was removed and the surface was sandblasted. Then, the cross section of the girder was restored with the same mortar mixture used for girders D and R-EXT. After the mortar cured, the NSM FRP strips were installed in accordance with the following procedure:

1. Grooves with the dimensions in Fig. 6 were cut into the concrete substrate using a tuckpointing grinder.

Deteriorated end region | Inserting NSM strips | Completed FRP repair

Figure 11. Progression of near-surface-mounted (NSM) fiber-reinforced polymer (FRP) repair for girder R-NSM.

2. Dust and debris were removed from the grooves using compressed air.

3. The grooves were partially filled with epoxy grout.

4. The FRP strips were inserted into the grooves using a sawing motion until the strips were centered at approximately the middepth of the groove.

5. The remainder of the grooves was filled with epoxy grout.

6. Excess grout was removed, and the surface was leveled using squeegees.

The transverse edge beam present in the bridge superstructure (Fig. 2) was unintentionally separated from girder R-NSM during extraction or transportation of the component. A portion of this edge beam remained on all of the other test girders (compare Fig. 11 with Fig. 10).

End block repair Minimal surface preparation was performed on girder R-BLK before the end block was constructed. **Figure 12** shows the state of the specimen after loose concrete was removed. Figure 12 also shows the reinforcing cage, which was fabricated in accordance with the details in Fig. 7, and the end block after construction was completed.

Experimental results

Table 4 summarizes the test results for the five girder specimens and corresponding material strengths. These results include the following:

- the maximum shear force resisted by the specimen V_{test}
- the ratio of the maximum shear resisted by the specimen to the maximum shear resisted by girder C $V_{test}/V_{control}$
- the ratio of the maximum shear resisted by the specimen to the maximum shear resisted by girder D $V_{test}/V_{damaged}$

To measure the strength of the precast concrete of each girder, at least three 4 × 6 in. (100 × 150 mm) concrete cores were taken from the webs of each specimen following the girder test. Table 4 provides the average compressive strength of the concrete cores f_c obtained from each girder in accordance with ASTM C42.[24] In addition, for specimens that received mortar repairs, Table 4 provides the compressive strength of the mortar f_m on the day of the girder tests, which was determined from 2 in. (50 mm) mortar cubes tested in accordance with

Deteriorated end region

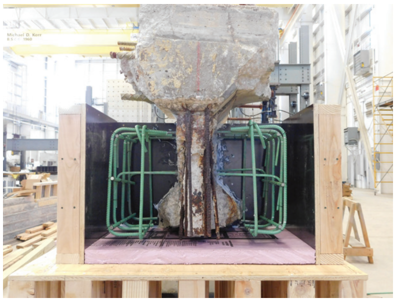

Completed reinforcing cage

Completed end block repair

Figure 12. Progression of end block repair for girder R-BLK.

Table 4. Summary of test results

Girder	f_c of cored concrete, ksi	f_m of mortar, ksi	f_c of end block concrete, ksi	f_{ct} of end block concrete, ksi	V_{test}, kip	$V_{test}/V_{control}$	$V_{test}/V_{damaged}$
C	7.27	n/a	n/a	n/a	141	1.00	1.76
D	9.24	9.13	n/a	n/a	80	0.57	1.00
R-EXT	7.44	16.10	n/a	n/a	189	1.34	2.36
R-NSM	9.07	12.17	n/a	n/a	31	0.22	0.39
R-BLK	7.85	n/a	7.07	0.63	81	0.57	1.01

Note: f_c = compressive strength of concrete; f_{ct} = splitting tensile strength of concrete; f_m = compressive strength of mortar; n/a = not applicable; $V_{control}$ = maximum shear resisted by girder C; $V_{damaged}$ = maximum shear resisted by girder D; V_{test} = maximum shear resisted by girder. 1 kip = 4.448 kN; 1 ksi = 6.895 MPa.

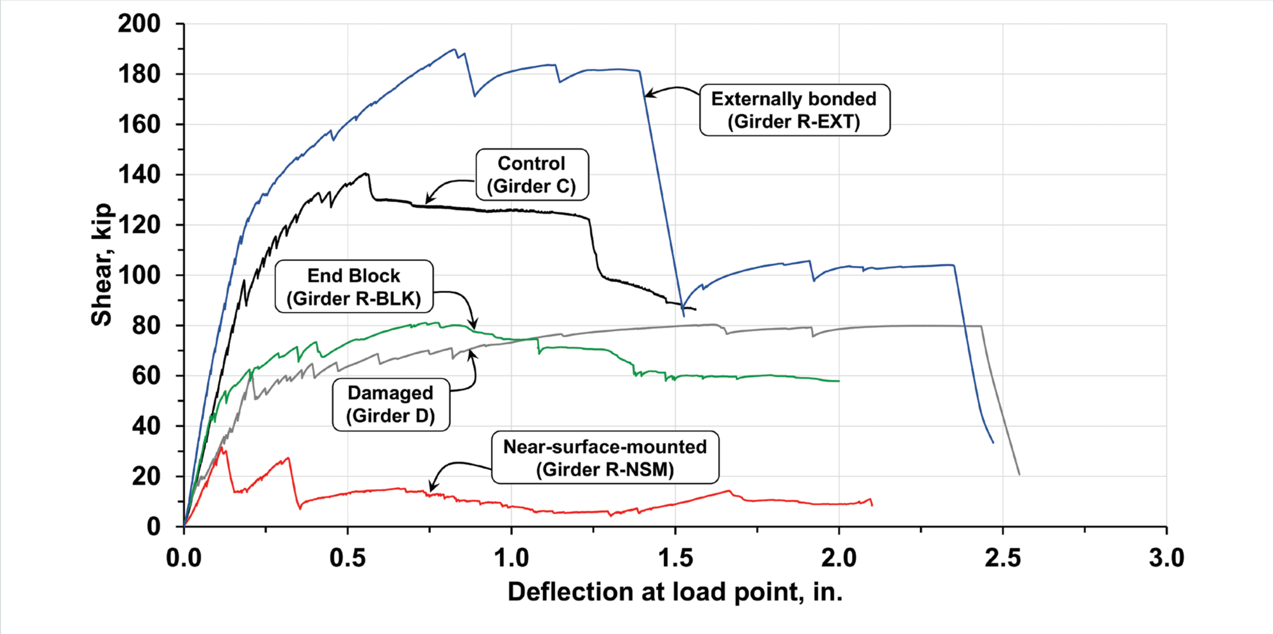

Figure 13. Shear versus deflection at load point for girder specimens. Note: 1 in. = 25.4 mm; 1 kip = 4.448 kN.

ASTM C109.[25] Finally, for girder R-BLK, Table 4 includes the compressive strength f_c and splitting tensile strength f_{ct} of the concrete of the end block obtained on the day of the girder test from 4 × 8 in. (100 × 200 mm) cylinders in accordance with ASTM C39[26] and ASTM C496,[27] respectively. Although variations in the compressive strengths of the concrete and mortar are evident among the girder specimens, these differences are not considered to be significant to the overall performance of the specimens based on the failure modes observed during the tests.

Figure 13 plots the shear within the test region (that is, the 45 in. [1140 mm] shear span) versus the deflection at the load point for each of the specimens. The shear due to the self-weight of the girder is not reflected in the response curves or the values in Table 4, but it is estimated to be approximately 6.5 kip (29 kN) at the middle of the 45 in. (1140 mm) shear span considering the original cross section of the girders. Deflections caused by deformation of the bearing pads were small (for example, deflection at the load point due to bearing pad deformation was 0.039 in. [0.99 mm] for girder C at V_{test}) and are therefore neglected.

Girder C

Failure of the control specimen was characterized by the formation of a diagonal strut within the test region, corresponding to a crack angle of approximately 43 degrees measured from horizontal (**Fig. 14**). Diagonal cracking developed in the web of the girder at a shear of 98 kip (440 kN). The primary diagonal crack did not extend to the support but instead extended to a point at the bottom of the girder located inside the span from the bearing region. This occurred due to the lack of development of the prestressing strands in the bottom flange near the end of the girder. The load-carrying capacity decreased as the diagonal cracks widened, and widening of the cracks corresponded with slippage of the prestressing strands in the bottom flange at the end of the girder. The ends of the strands slipped approximately 1.25 in. (31.8 mm) into the girder by the end of the test. The relatively sudden loss in load-carrying capacity observed at a deflection of 1.24 in. (31.5 mm) was likely due to strand slip.

Girder D

For the damaged specimen, the primary failure crack (Fig. 14) initiated at the bottom of the component approximately 42 in. (1070 mm) from the end of the specimen at a shear of 61 kip (270 kN), propagated vertically through the web upon further loading, and finally propagated diagonally through the top flange and deck toward the load point. Failure was defined by an abrupt drop in the load-carrying capacity at a deflection of 2.43 in. (61.7 mm) (Fig. 13). By the end of the test, portions of the bottom flange on both sides of the web had detached from the specimen at the support (Fig. 14). This separation of the bottom flange began early in the test due to the deteriorated state of the girder. As indicated in Table 4, the ratio of the shear capacity of girder D to the capacity of girder C is 0.57.

Girder R-EXT

Figure 13 shows that girder R-EXT exhibited an initial stiffness greater than that of girder C. As load was increased, the behavior of the specimen became dominated by the opening of a flexural crack located at the termination of the longitudinal FRP strips (approximately 49 in. [1240 mm] from the end

Control specimen (girder C)

Damaged specimen (girder D)

Figure 14. Control and damaged specimens after failure.

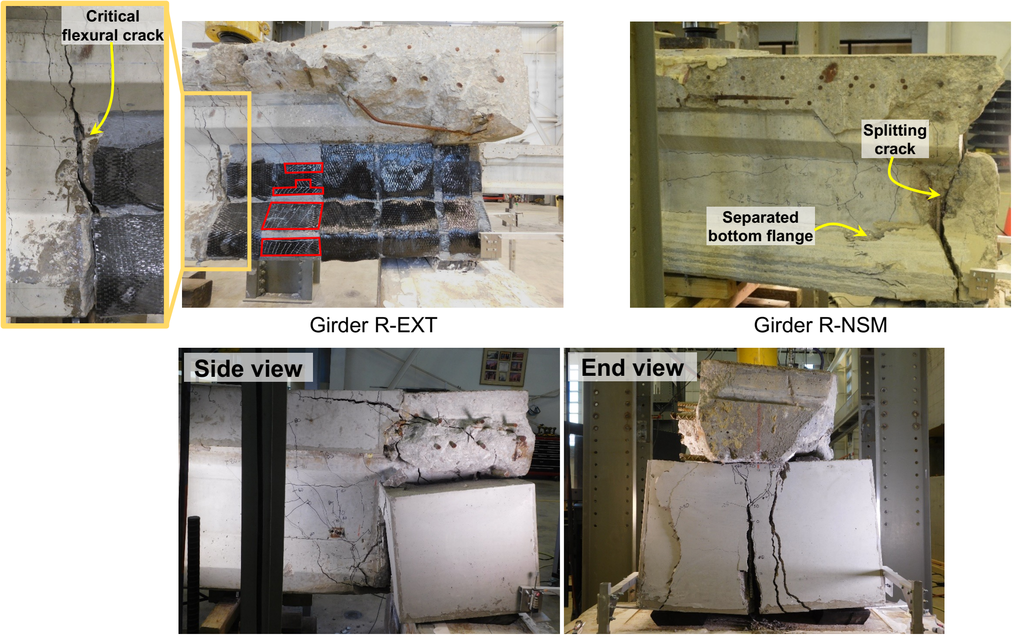

Girder R-EXT

Girder R-NSM

Girder R-BLK

Figure 15. Repaired girders after failure.

of the girder). This primary flexural crack was first visually observed at a shear of 140 kip (620 kN) but may have initiated earlier; close visual examination of the specimen was not conducted at high loads because of safety concerns. During the test, relatively minor diagonal cracking also developed near the load point in the region not covered by FRP reinforcement; however, the portions of the diagonal cracks that were visible did not widen significantly after their formation. Propagation of the cracks toward the support is unknown because of the presence of the FRP.

Figure 15 shows girder R-EXT after failure. The specimen experienced a flexural failure characterized by complete fracture of two prestressing strands in the bottom flange at the wide critical flexural crack (Fig. 15), which was located at the termination of the longitudinal FRP strips. Based on observations during the test, the sudden losses in load-carrying capacity that occurred at a deflection of 1.39 in. (35.3 mm) and a deflection of 2.35 in. (59.7 mm) correspond with the strand fractures (Fig. 13). The externally bonded FRP prevented failure from occurring within the repaired region.

Failure instead occurred outside the deteriorated region of the girder.

Minimal FRP debonding from the concrete surface was observed after testing. It was confined to areas along the longitudinal strips that were not directly covered with patches or vertical FRP sheets. Figure 15 outlines the debonded areas on one side of the girder in red. No rupture of the FRP occurred.

Girder R-NSM

At the beginning of the test on girder R-NSM, the girder's initial stiffness was less than that of the other specimens (Fig. 13). Relatively early in the test, when a shear of 31 kip (140 kN) was reached, the portion of the web located above the support bearing experienced a splitting crack that effectively caused the end of the specimen to separate from the rest of the girder (Fig. 15). The splitting crack appeared suddenly over the depth of the girder, intersecting with the reentrant corner at the notch located along the top flange of the girder, and resulted in a sudden loss in load-carrying capacity. Once the end of the specimen that separated from the rest of the girder was no longer effective in transferring load to the bearing, the reaction force was primarily transferred through a relatively small portion of the bottom flange in contact with the bearing pad. After reaching a second peak in the response curve, load-carrying capacity was again lost when the outer portions of the bottom flange separated from the girder at a shear of 27 kip (120 kN) (Fig. 15). Because of the premature failure, the NSM strips were not effectively engaged.

As previously discussed, girder R-NSM lacked a portion of the transverse edge beam of the bridge superstructure that was present on the other specimens (Fig. 2). The absence of a portion of this edge beam may have contributed to the splitting observed in the vicinity of the notch during the test.

Girder R-BLK

The response curve of girder R-BLK presents an initial stiffness similar to that of girder C (Fig. 13). As loading increased, the end face of the girder R-BLK end block began to experience minor cracking at a shear of 8.9 kip (40 kN). At a shear of 44 kip (200 kN), cracking had propagated vertically through the full depth of the end block and extended longitudinally along the bottom of the block. This cracking led to the block eventually splitting into two pieces (Fig. 15). Outside of the end block, a diagonal crack initiated at a shear of approximately 53 kip (240 kN). Diagonal cracking extended from the bottom surface of the girder near the edge of the end block toward the load point, indicating the development of a diagonal strut. The load test was terminated after the interface between the end block and the original girder failed (that is, the end block separated for the concrete of the original girder), and the end block experienced significant rotation relative to the girder (Fig. 15).

Analysis of results

A diagonal strut developed within the test region of the control girder (girder C) (Fig. 14); however, the damaged girder (girder D) exhibited behavior governed by the inability of the corroded prestressing strands to develop sufficient tensile force along the bottom flange at the end of the component. A diagonal strut could not form within the test region without adequate tensile capacity along the bottom flange to equilibrate the horizontal component of the strut. The primary failure crack of the damaged specimen was nearly vertical. The behaviors of the control and damaged specimens clearly indicate the importance of the tensile capacity along the bottom flange in developing the full strength of the girder.

The test results present a distinction between the satisfactory performance achieved by the specimen with externally bonded FRP and issues for the specimens with the NSM FRP and end block repair systems that prevented the girders from achieving restoration of the strength and stiffness of the damaged end regions. For girder R-NSM, the maximum shear V_{test} resisted by the specimen was only 22% of the shear resisted by girder C and 39% of the shear resisted by girder D. Although the lack of a portion of the transverse edge beam on the specimen may have negatively affected specimen performance, the splitting above the support bearing demonstrates the importance of providing adequate confinement within the region of the girder repaired with mortar. Because the NSM strips were not effectively engaged, the behavior of the specimen essentially represents the performance of a girder repaired only with mortar and highlights the need to provide strengthening measures beyond simply restoring the cross section of the girder using a fast-setting mortar.

Girder R-BLK achieved a maximum shear V_{test} that was only 57% of the strength of girder C and essentially equal to the strength of girder D. Although the initial stiffness of girder R-BLK was similar to that of girder C, its postcracking behavior more closely resembled the behavior of girder D. Cracking and loss of stiffness occurred at a relatively low shear, causing the linear portion of the response curve to end at a shear of 44 kip (200 kN), less than half the shear achieved by girder C before diagonal crack formation (98 kip [440 kN]). The formation of cracks in girder R-BLK at a low shear was caused by the elimination of the original center bearing, which forced the load to be transferred through the end block to the two new bearing areas. Furthermore, the absence of continuous reinforcement near the bottom (that is, along the tension face) of the end block transverse to the longitudinal axis of the girder caused the splitting of the end block to quickly increase in severity upon further loading due to the absence of a tension tie. Continuous reinforcement with proper development is essential for a successful end block repair to properly transfer stresses to the bearing pads supporting the end block and to control any cracks that develop. The end block essentially behaved as an unreinforced deep transfer beam.

The externally bonded FRP repair system of girder R-EXT provided a shear capacity that exceeded the capacity of girder C by 34%. Furthermore, the linear portion of the response curve ends at a shear that is 17% greater than the shear when diagonal cracking developed in girder C. Because of the high stiffness of the FRP laminate material, the repair system was able to restore the stiffness lost due to the deterioration of the end region, providing a greater initial stiffness than that of the control specimen. Considering that a flexural failure outside of the repaired region was achieved, the externally bonded FRP repair system was able to restore shear capacity within the deteriorated end region, reestablish the tie force in the bottom flange that was lost due to deterioration that caused the failure behavior exhibited by girder D, and provide sufficient confinement to the region repaired with mortar. The confinement provided by the FRP prevented any splitting above the support bearing as observed for girder R-NSM, and it precluded separation of portions of the bottom flange of the component as experienced by girders D and R-NSM. Moreover, the confinement allowed two strands to reach their ultimate rupture strengths at the end of the repaired region and prevented the significant slip of the strands observed during the test on girder C.

Considering that the NSM strips in girder R-NSM were not effectively engaged due to premature splitting of the repaired region, the addition of externally bonded FRP to confine the end region and prevent such splitting may allow NSM strips to provide tensile capacity along the bottom flange. Such a hybrid repair system that incorporates both NSM strips in the bottom flange and externally bonded FRP reinforcement could be a viable technique for restoring the strength and stiffness of a deteriorated end region and deserves further study.

Conclusion

The primary conclusions resulting from the experimental investigation conducted to evaluate repair techniques for prestressed concrete bridge girders with severe end region deterioration are as follows:

- Deterioration of the end regions of prestressed concrete girders can result in significant reductions in strength (43% or greater shear strength reduction considering results of the control and damaged specimens).

- When designing end region repair systems for prestressed concrete girders, it is critical to restore the tensile capacity lost due to corroded and ineffective prestressing strands in the bottom flange of the deteriorated end regions. Without adequate tensile capacity in the bottom flange, a diagonal strut cannot form within the end region, resulting in premature failure and decreased capacity.

- It is also critical to ensure that confinement of the repair material (for example, mortar) used to restore the cross section of the girder is adequate. End confinement, such as the confinement provided by externally bonded longitudinal FRP strips, is needed to prevent the premature splitting failure mode observed during the test on the specimen with NSM FRP reinforcement. Providing confinement around the repaired region also mitigates some concerns about the condition of the concrete at the interface between the original girder concrete and repair material, as well as concerns about the resulting bond between the two materials.

- The externally bonded FRP repair system proved to be a viable technique for restoring the strength and stiffness of the prestressed concrete girder with severe end region deterioration. The repaired specimen achieved a greater shear capacity and a greater initial stiffness than the control specimen, leading to a flexural failure outside of the repaired region. The chosen spike anchor details were successful in preventing FRP failure due to debonding.

- The NSM FRP repair system did not provide adequate confinement to the region repaired with mortar; therefore, the strength and stiffness of the prestressed concrete bridge girder were not restored. If NSM strips are installed along the vertical and sloped surfaces of the bottom flange as a strengthening measure, additional consideration should be given to confining the portion of the girder that is restored using a repair material.

- The end block system also did not reestablish the strength of the deteriorated end region, though the system restored the initial stiffness of the component. Elimination of the original bearing under the girder web and the absence of continuous transverse reinforcement along the bottom of the end block to aid with transferring stresses to the new support areas resulted in premature failure. Therefore, the failure prevented evaluation of the potential benefit of this approach.

With modifications, the NSM FRP and end block repair systems could potentially be viable techniques to restore the behavior of prestressed concrete girders with end region deterioration. Further research, however, is needed to evaluate the success of modified versions of these repair systems.

Acknowledgments

This work was supported by the Joint Transportation Research Program administered by the Indiana Department of Transportation and Purdue University. The authors would like to thank the members of the Study Advisory Committee for providing guidance and direction for the research. Appreciation is also extended to Sika Corp., Pilgrim Permacoat, and Owens Corning for their assistance with material acquisition for the experimental program. The contents of this paper reflect the views of the authors, who are responsible for the facts and accuracy of the data presented herein and do not necessarily reflect the official views or policies of the sponsoring organization. These contents do not constitute a standard, specification, or regulation.

References

1. Andrawes, B., I. D. Shaw, and H. Zhao. 2018. *Repair and Strengthening of Distressed/Damaged Ends of Prestressed Beams with FRP Composites*. Report FHWA-ICT-18-001. Urbana, IL: Illinois Center for Transportation, University of Illinois at Urbana-Champaign. https://doi.org/10.36501/0197-9191/18-001.

2. Floyd, R. W., J. S. Volz, T. Looney, M. Mesigh, M. Ahmadi, S. Roswurm, P. Huynh, and M. Manwarren. 2021. *Evaluation of Ultra-High Performance Concrete, Fiber Reinforced Self-Consolidating Concrete, and MALP Concrete for Prestressed Girder Repair*. Report FHWA-OK-21-03. Oklahoma City, OK: Oklahoma Department of Transportation. https://shareok.org/handle/11244/330981.

3. Needham, D. E. 1999. *Prestressed Concrete Beam End Repair (Interim Report)*. Report R-1373. Lansing: Michigan Department of Transportation. https://mdotjboss.state.mi.us/SpecProv/getDocumentById.htm?docGuid=bcf5caef-cd66-4f6c-91c6-5bc1e86c1ab8.

4. Needham, D. E. 2000. *Prestressed Concrete Beam End Repair (Final Report)*. Report R-1380. Lansing, MI: Michigan Department of Transportation. https://mdotjboss.state.mi.us/SpecProv/getDocumentById.htm?docGuid=b47813a4-cafe-4d32-b4fd-51cee10d7b9e.

5. Petty, D. A., P. J. Barr, P. G. Osborn, M. W. Halling, and T. R. Brackus. 2011. "Carbon Fiber Shear Retrofit of Forty-Two-Year-Old AASHTO I-Shaped Girders." *Journal of Composites for Construction* 15 (5): 773–781. https://doi.org/10.1061/(ASCE)CC.1943-5614.0000208.

6. Ramseyer, C., and T. H.-K. Kang. 2012. "Post-Damage Repair of Prestressed Concrete Girders." *International Journal of Concrete Structures and Materials* 6 (3): 199–207. https://doi.org/10.1007/s40069-012-0019-7.

7. Shafei, B., B. Phares, and S. Weizhuo. 2020. *Beam End Repair for Prestressed Concrete Beams*. Report IHRB Project TR-715. Ames, IA: Bridge Engineering Center, Iowa State University. http://publications.iowa.gov/33803/1/TR-715_Final%20Report_Beam%20End%20Repair%20for%20Prestressed%20Concrete%20Beams.pdf.

8. Shield, C., and P. Bergson. 2018. *BR27568—Experimental Shear Capacity Comparison between Repaired and Unrepaired Girder Ends*. Report MN/RC 2018-07. Minneapolis, MN: Minnesota Department of Transportation. http://www.dot.state.mn.us/research/reports/2018/201807.pdf.

9. American Concrete Institute (ACI) Committee 440. 2017. *Guide for the Design and Construction of Externally Bonded FRP Systems for Strengthening Concrete Structures*. ACI PRC-440.2R-17. Farmington Hills, MI: ACI.

10. Cai, C. S, and M. Xia. 2015. *Repairing/Strengthening of Bridges with Post-Tensioned FRP Materials and Performance Evaluation*. Report FHWA/LA.11/488. Baton Rouge, LA: Louisiana Transportation Research Center, Louisiana Department of Transportation and Development. https://rosap.ntl.bts.gov/view/dot/29399.

11. Pevey, J. M., W. B. Rich, C. S. Williams, and R. J. Frosch. 2021. *Repair and Strengthening of Bridges in Indiana Using Fiber Reinforced Polymer Systems: Volume 1–Review of Current FRP Repair Systems and Application Methodologies*. Report FHWA/IN/JTRP-2021/09. West Lafayette, IN: Joint Transportation Research Program, Purdue University. https://doi.org/10.5703/1288284317309.

12. Rich, W. B., R. R. Jacobs, C. S. Williams, and R. J. Frosch. 2021. *Repair and Strengthening of Bridges in Indiana Using Fiber Reinforced Polymer Systems: Volume 2–FRP Flexural Strengthening and End Region Repair Experimental Programs*. Report FHWA/IN/JTRP-2021/10. West Lafayette, IN: Joint Transportation Research Program, Purdue University. https://doi.org/10.5703/1288284317310.

13. Pei, J. S., R. D. Martin, C. J. Sandburg, and T. H.-K. Kang. 2008. *Rating Precast Prestressed Concrete Bridges for Shear*. Report FHWA-OK-08-08. Oklahoma City, OK: Oklahoma Department of Transportation. https://www.odot.org/hqdiv/p-r-div/spr-rip/library/reports/fhwa-ok0808.pdf.

14. Indiana Department of Highways. 1987. *Bridge Plans for Spans over 20 Feet on State Road No. 24 (Project No. MAF-170-1)*. Indianapolis, IN: Indiana Department of Highways.

15. Ghannoum, W. M., N. K. Alotaibi, J. Garcia, C. H. Kim, Y. Kim, D. Pudleiner, K. Quinn, N. Satrom, W. Shekarchi, W. Sun, H. Wang, and J. Jirsa. 2018. "Shear Strengthening of Concrete Bridges Using CFRP Strips and Anchors and Quality Control Procedures." *ACI Symposium Publication* 327: 43.1–43.20. https://doi.org/10.14359/51713364.

16. Shekarchi, W. A., D. K. Pudleiner, N. K. Alotaibi, W. M. Ghannoum, and J. O. Jirsa. 2020. "Carbon Fiber-Reinforced Polymer Spike Anchor Design Recommendations." *ACI Structural Journal* 117 (6): 171–182. https://doi.org/10.14359/51728065.

17. Pudleiner, D. K. 2016. "Design Considerations Based on Size Effects of Anchored Carbon Fiber Reinforced Polymer (CFRP) Systems." MS thesis, University of Texas at Austin. http://hdl.handle.net/2152/39031.

18. Kim, Y. G. 2011. "Shear Behavior of Reinforced Con-

crete T-Beams Strengthened with Carbon Fiber Reinforced Polymer (CFRP) Sheets and CFRP Anchors." PhD dissertation, University of Texas at Austin. http://hdl.handle.net/2152/ETD-UT-2011-12-4398.

19. Orton, S. L. 2007. "Development of a CFRP System to Provide Continuity in Existing Reinforced Concrete Buildings Vulnerable to Progressive Collapse." PhD dissertation, University of Texas at Austin. http://hdl.handle.net/2152/3241.

20. ASTM International. 2018. *Standard Specification for Deformed and Plain Carbon-Steel Bars for Concrete Reinforcement*. ASTM A615/A615M-18. West Conshohocken, PA: ASTM International. https://doi.org/10.1520/A0615_A0615M-18.

21. ASTM International. 2019. *Standard Specification for Portland Cement*. ASTM C150/C150M-19a. West Conshohocken, PA: ASTM International. https://doi.org/10.1520/C0150_C0150M-19A.

22. ASTM International. 2019. *Standard Specification for Coal Fly Ash and Raw or Calcined Natural Pozzolan for Use in Concrete*. ASTM C618-19. West Conshohocken, PA: ASTM International. https://doi.org/10.1520/C0618-19.

23. ICRI (International Concrete Repair Institute) Committee 310. 2013. *Selecting and Specifying Concrete Surface Preparation for Sealers, Coatings, Polymer Overlays, and Concrete Repair*. ICRI Guideline 310.2R-2013. Rosemont, IL: ICRI.

24. ASTM International. 2019. *Standard Test Method for Obtaining and Testing Drilled Cores and Sawed Beams of Concrete*. ASTM C42/C42M-18a. West Conshohocken, PA: ASTM International. https://doi.org/10.1520/C0042_C0042M-18A.

25. ASTM International. 2016. *Standard Test Method for Compressive Strength of Hydraulic Cement Mortars (Using 2-in. or [50-mm] Cube Specimens)*. ASTM C109/C109M-16a. West Conshohocken, PA: ASTM International. https://doi.org/10.1520/C0109_C0109M-16A.

26. ASTM International. 2018. *Standard Test Method for Compressive Strength of Cylindrical Concrete Specimens*. ASTM C39/C39M-18. West Conshohocken, PA: ASTM International. https://doi.org/10.1520/C0039_C0039M-18.

27. ASTM International. 2017. *Standard Test Method for Splitting Tensile Strength of Cylindrical Concrete Specimens*. ASTM C496/C496M-17. West Conshohocken, PA: ASTM International. https://doi.org/10.1520/C0496_C0496M-17.

Notation

E_f = tensile modulus of elasticity of fiber-reinforced polymer reinforcement reported by manufacturer

f_c = compressive strength of concrete

f'_c = specified 28-day concrete compressive strength

f_{ct} = splitting tensile strength of concrete

f_{fu}^* = ultimate tensile strength of fiber-reinforced polymer reinforcement reported by manufacturer

f_m = compressive strength of mortar

f_{pu} = ultimate tensile strength of prestressing strand

$V_{control}$ = maximum shear force resisted by girder C

$V_{damaged}$ = maximum shear force resisted by girder D

V_{test} = maximum shear force resisted by girder

ε_{fu}^* = ultimate rupture strain of fiber-reinforced polymer reinforcement reported by manufacturer

About the authors

William B. Rich, MS, is a structural engineer at Martin/Martin in Denver, Colo. He received his bachelor's degree in civil engineering from the University of Wyoming in Laramie and his master's degree from Purdue University in West Lafayette, Ind.

Christopher S. Williams, PhD, is an assistant professor of civil engineering at Purdue University. He received his bachelor's degree in civil engineering from Southern Illinois University Carbondale and his master's and PhD degrees from the University of Texas at Austin.

Robert J. Frosch, PhD, PE, FACI, FASCE, is a professor of civil engineering and vice provost for academic facilities at Purdue University. A fellow of the American Concrete Institute and American Society of Civil Engineers, he is the editor-in-chief of the *ACI Structural Journal* and serves on the ACI 318 Structural Concrete Building Code Committee, for which he chairs ACI 318D, Structural Members. His research, which focuses on the design and behavior of structural concrete, has resulted in changes to the ACI building code and the American Association of State Highway and Transportation Officials' design specifications.

Abstract

Deterioration of the end regions of prestressed concrete bridge girders is commonly observed in the field when girders are exposed to chloride-laden water that has leaked through failed expansion joints. Because the deterioration is often localized to the end regions of the girders, reliable repair techniques can provide a means to extend girder service life, avoiding the need for immediate superstructure replacement. To evaluate different repair methods and identify key design considerations for end region repair, shear tests to failure were conducted on prestressed concrete girders extracted from a decommissioned superstructure. Three repair systems were evaluated: an externally bonded fiber-reinforced-polymer (FRP) system, a near-surface-mounted FRP system, and a concrete end block. Only the externally bonded FRP system successfully restored both the strength and initial stiffness of the girder. Although the other two methods were not successful, the tests on the repaired girders highlight important factors that must be considered when designing repairs or conducting further research. The tests also demonstrate that end region deterioration can cause significant (> 40%) reductions in strength, underscoring the importance of addressing such deterioration observed in the field.

Keywords

Corrosion, bridge, end region repair, externally bonded reinforcement, fiber-reinforced polymer, FRP, girder, near-surface-mounted reinforcement, NSM, prestressed concrete bridge girders, shear strengthening.

Review policy

This paper was reviewed in accordance with the Precast/Prestressed Concrete Institute's peer-review process. The Precast/Prestressed Concrete Institute is not responsible for statements made by authors of papers in *PCI Journal*. No payment is offered.

Publishing details

This paper appears in *PCI Journal* (ISSN 0887-9672) V. 68, No. 2, March–April 2023, and can be found at https://doi.org/10.15554/pcij68.2-02. *PCI Journal* is published bimonthly by the Precast/Prestressed Concrete Institute, 8770 W. Bryn Mawr Ave., Suite 1150, Chicago, IL 60631.

Reader comments

Please address any reader comments to *PCI Journal* editor-in-chief Tom Klemens at tklemens@pci.org or Precast/Prestressed Concrete Institute, c/o *PCI Journal*, 8770 W. Bryn Mawr Ave., Suite 1150, Chicago, IL 60631.